Inorg. Chem. **2007**, *46*, 48–59

Weak-Field Anions Displace the Histidine Ligand in a Synthetic Heme Peptide but Not in *N*-Acetylmicroperoxidase-8: Possible Role of Heme Geometry Differences

Aaron B. Cowley and David R. Benson*

Department of Chemistry, University of Kansas, Lawrence, Kansas 66045

Received April 21, 2006

We have recently reported that aquo and thioether complexes of the ferric cytochrome *c* heme peptide *N*-acetylmicroperoxidase-8 (Fe^{III}-**1**) exhibit greater low-spin character than do the corresponding complexes of a synthetic, water-soluble, monohistidine-ligated heme peptide (Fe^{III}-**2**; Cowley, A. B.; Lukat-Rodgers, G. S.; Rodgers, K. R.; Benson, D. R. *Biochemistry* **2004**, *43*, 1656–1666). Herein we report results of studies showing that weak-field ligands bearing a full (fluoride, chloride, hydroxide) or partial (phenoxide, thiocyanate) negative charge on the coordinating atom trigger dissociation of the axial His ligand in Fe^{III}-**2** but not in Fe^{III}-**1**. We attribute the greater sensitivity of His ligation in Fe^{III}-**1** to weak-field anionic ligands than to weak-field neutral ligands to the following phenomena: (1) anionic ligands pull Fe^{III} further from the mean plane of a porphyrin than do neutral ligands, which will have the effect of straining the His–Fe bond in Fe^{III}-**2**, and (2) heme in Fe^{III}-**2** is likely to undergo a modest doming distortion following anion binding that will render the His-ligated side of the porphyrin concave, thereby increasing porphyrin/ligand steric interactions. We propose that ruffling of the heme in Fe^{III}-**1** is an important factor contributing to its ability to resist His dissociation by weak-field anions. First, ruffling should allow His to more closely approach the porphyrin than is possible in Fe^{III}-**2**, thereby reducing bond strain following anion binding. Second, the ruffling deformation in Fe^{III}-**1**, which is enforced by the double covalent heme–peptide linkage, will almost certainly prevent significant porphyrin doming.

Introduction

Heme in mitochondrial cytochrome *c* is covalently linked to the polypeptide via thioether bonds between its vinyl groups and cysteine residues 14 and 17 in a conserved $Cys^{14}-Xaa^{15}-Xaa^{16}-Cys^{17}-His^{18}$ motif. The imidazolyl side chain of histidine-18 (His-18) occupies one of the axial ligation sites of iron, and the thioether side chain of methionine-80 (Met-80) serves as the second axial ligand. Proteolysis of horse cytochrome *c* (cyt *c*) by pepsin and trypsin[1] followed by acetylation of the peptide N-terminus[2−4] generates heme octapeptide **1**, commonly referred to as

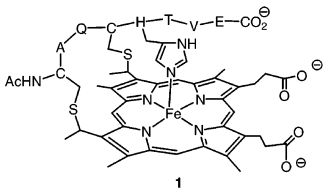

1

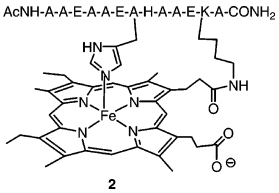

2

N-acetylmicroperoxidase-8 because it mimics the catalytic activity of heme peroxidases.[5,6]

Several key structural features of horse cyt *c* are retained in **1** at neutral pH, including (1) the double covalent heme−polypeptide linkage, (2) His-18 being an axial ligand to iron, (3) a single turn of 3_{10}-helix spanning the covalently attached Cys residues virtually identical to that in cyt *c*, as determined in NMR studies of the low-spin cyanide complex,[7] (4) high

* To whom correspondence should be addressed. Phone: (785)-864-4090. Fax: (785)-864-5396. E-mail: drb@ku.edu.

(1) Harbury, H. A.; Loach, P. A. *J. Biol. Chem.* **1960**, *235*, 3646−3653.
(2) Munro, O. Q.; Marques, H. M. *Inorg. Chem.* **1996**, *35*, 3752−3767.
(3) Wang, J.-S.; VanWart, H. E. *J. Phys. Chem.* **1989**, *93*, 7925−7931.
(4) Yang, E. K.; Sauer, K. Correlation between the optical and magnetic properties of ferric *N*-acetylated heme octapeptide complexes. In *Electron Transport and Oxygen Utilization*; Ho, C., Ed.; Elsevier: Amsterdam, 1982; p 82.
(5) Adams, P. A. *J. Chem. Soc. Perkin Trans. 2* **1990**.
(6) Adams, P. A. In *Peroxidases in Chemistry and Biology*; Everse, J., Grisham, M. B., Eds.; CRC Press: Boca Raton, FL, 1990; Vol. 2, Chapter 7.
(7) Low, D. W.; Gray, H. B.; Duus, J. O. *J. Am. Chem. Soc.* **1997**, *119*, 1−5.

10.1021/ic060682c CCC: $37.00
Published on Web 12/09/2006

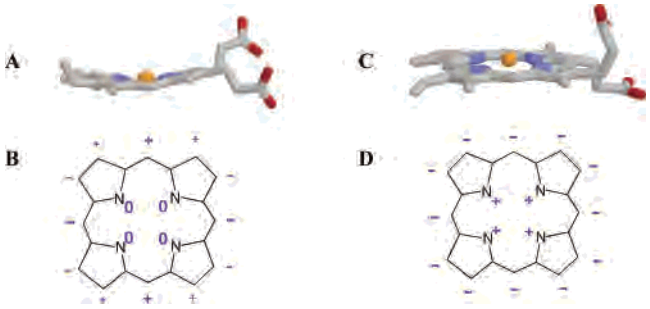

Figure 1. Ruffled heme from horse heart cytochrome *c* (A) and domed heme from sperm whale myoglobin (B); also shown are schematic drawings indicating displacements of the porphyrin atoms relative to the mean plane for ideally ruffled (C) and ideally domed (D) distortions.

solubility in water; and (5) nonplanar distortion of the heme (Figure 1A) which consists mainly of ruffling.[8−11] In an ideally ruffled heme, the meso carbons lie alternately above (+) and below (−) the mean porphyrin plane (Figure 1B), but the four pyrrole nitrogens comprising the equatorial coordination sphere of iron remain in the plane. Experimental[11] and computational[9] studies with ferric **1** (Fe^{III}-**1**) have indicated that heme ruffling substantially diminishes when the His−Fe bond dissociates. We have recently reported far-UV circular dichroism (CD) spectroscopic data showing that His−Fe bond dissociation in **1** also results in complete loss of peptide secondary structure. On the basis of these observations, we concluded that His−Fe ligation, induction of peptide secondary structure, and heme ruffling in **1** occur a single cooperative transition.[12]

Heme peptide **2** and its isomeric relatives, developed in our laboratories,[13,14] were the first synthetic monohistidine-ligated heme peptides reported in the literature which, like **1** and its relatives, are soluble in water.[12] Heme peptide **2** shares a number of other features with **1** that make it ideal for comparative studies,[12] including (1) a solvent molecule occupying the second axial coordination site, as indicated by resonance Raman (rR) spectra recorded in 1:1 H_2O/CH_3OH,[12] (2) peptide secondary structure (∼50% α-helix) that is induced by His−Fe ligation,[13] (3) a porphyrin of similar electronic character (mesoheme is considered a reasonable model of heme *c*[15]), and (4) an identical overall charge of −3 at neutral pH, not counting the formal positive charge on Fe^{III}. Heme peptides **1** and **2** also exhibit some key differences. First, the heme−peptide linkage in **2** comprises a single amide bond between a lysine side chain and a mesoheme propionate group and is therefore much more flexible than the double covalent linkage in **1**. Second, rR spectroscopic data have revealed that structure-sensitive but substituent-insensitive vibrational bands υ_2 and υ_4 occur 2−3 cm^{-1} lower in frequency in Fe^{III}-**1** than in Fe^{III}-**2**, providing clear evidence for more extensive heme ruffling in the former.[12] In fact, we consider it likely that heme in Fe^{III}-**2** is essentially planar. This difference in heme geometry appears to explain why Fe^{III}-**2** is much more prone toward self-association than is Fe^{III}-**1**:[12] a planar heme has a much greater surface area available for intermolecular interactions than does a ruffled heme.[16] Finally, rR[12,17] and EPR data[12,18] indicated that Fe^{III}-**1** is in equilibrium between high-spin (predominantly $S = 5/2$) and low-spin ($S = 1/2$) states but that Fe^{III}-**2** is almost fully high-spin.[12] We therefore have a relatively rare situation in which two coordination complexes share identical equatorial and axial ligands, but with the metal ion in one of them (Fe^{III}-**1**) experiencing a considerably stronger ligand field. An interesting consequence of this phenomenon arose when we attempted to compare the abilities of Fe^{III}-**1** and Fe^{III}-**2** to recapitulate the low-spin Met/His ligation exhibited by ferric cyt *c*, using the thioether 2-(methylthio)ethanol (MTE; $CH_3SCH_2CH_2OH$) as a Met-80 analogue. As anticipated on the basis of previously reported studies with cyt *c* heme peptides,[4,17,19] displacement of the aquo ligand in Fe^{III}-**1** by MTE was slightly exergonic and yielded a low-spin complex (Table 1).[12] In contrast, reaction between MTE and Fe^{III}-**2** was slightly endergonic and yielded a complex with no detectable low-spin character.[12] Both Fe^{III}-**1** and Fe^{III}-**2** formed low-spin 1:1 complexes with the stronger nitrogenous ligands imidazole (Im; a model for a His side chain) and glycine (Gly; a model for the protein N-terminus).[12]

On the basis of the following observations in our previously published study, we concluded that the stronger ligand fields experienced by iron in the MTE and aquo complexes of Fe^{III}-**1** than of Fe^{III}-**2** are due, at least in part, to stronger ligand binding:[12] (1) pH titration experiments revealed that Fe^{III}-**1** is ∼0.7 kcal/mol more stable than Fe^{III}-**2** with respect to axial His ligand dissociation. Somewhat greater stability of Fe^{III}-**1** relative to Fe^{III}-**2** (1.4 kcal/mol) was suggested by studies in which the axial His ligand in the low-spin imidazole complex of each species was displaced by a second equivalent of imidazole. (2) MTE binds ∼0.5 kcal/mol more strongly to Fe^{III}-**1** than to Fe^{III}-**2** (Table 1). (3) Lowering the temperature from 25 to 5 °C in a solution containing Fe^{III}-**2**(MTE) introduced ∼50% low-spin character, as determined by UV/vis spectroscopy. The decrease in temperature increases the strength of His−Fe ligation and should also increase the free energy of MTE binding.

(8) Laberge, M.; Vreugdenhil, A. J.; Vanderkooi, J. M.; Butler, I. S. *J. Biomol. Struct. Dyn.* **1998**, *15*, 1039−1050.
(9) Ma, J.-G.; Laberge, M.; Song, X.-Z.; Jentzen, W.; Jia, S.-L.; Zhang, J.; Vanderkooi, J. M.; Shelnutt, J. A. *Biochemistry* **1998**, *37*, 5118−5128.
(10) Melchionna, S.; Barteri, M.; Ciccotti, G. *J. Phys. Chem.* **1996**, *100*, 19241−19250.
(11) Othman, S.; Le Lirzin, A.; Desbois, A. *Biochemistry* **1994**, *33*, 15437−15448.
(12) Cowley, A. B.; Lukat-Rodgers, G. S.; Rodgers, K. R.; Benson, D. R. *Biochemistry* **2004**, *43*, 1656−1666.
(13) Arnold, P. A.; Benson, D. R.; Brink, D. J.; Hendrich, M. P.; Jas, G. S.; Kennedy, M. L.; Petasis, D. T.; Wang, M. *Inorg. Chem.* **1997**, *36*, 5306−5315.
(14) Benson, D. R.; Hart, B. R.; Zhu, X.; Doughty, M. B. *J. Am. Chem. Soc.* **1995**, *117*, 8502−8510.
(15) Shifman, J. M.; Gibney, B. R.; Sharp, R. E.; Dutton, P. L. *Biochemistry* **2000**, *39*, 14813−14821.
(16) Alden, R. G.; Ondrias, M. R.; Shelnutt, J. A. *J. Am. Chem. Soc.* **1990**, *112*, 691−697.
(17) Tezcan, F. A.; Winkler, J. R.; Gray, H. B. *J. Am. Chem. Soc.* **1998**, *120*, 13383−13388.
(18) Munro, O. Q.; de Wet, M.; Pollak, H.; van Wyk, J.; Marques, H. M. *J. Chem. Soc. Faraday Trans.* **1998**, *94*, 1743−1752.
(19) Harbury, H. A.; Cronin, J. R.; Fanger, M. W.; Hettinger, T. P.; Murphy, A. J.; Myer, Y. P.; Vinogradov, S. N. *Proc. Natl. Acad. Sci. U.S.A.* **1965**, *54*, 1658−1664.

Table 1. Ligand Binding Data

compd	ligand	K_{eq} M^{-1}	$\Delta G°$ kcal/mol	$\Delta H°$ kcal/mol	$\Delta S°$ cal/mol K
Fe^{III}-**1**	ImH	5495 ± 172	-5.1 ± 0.2	-16.3 ± 0.6	-37.2 ± 1.7
Fe^{III}-**2**		6789 ± 165	-5.2 ± 0.2	-14.8 ± 0.7	-32.2 ± 1.3
Fe^{III}-**1**	MTE	1.2 ± 0.1	-0.2 ± 0.1		
Fe^{III}-**2**		0.6 ± 0.1	$+0.3 \pm 0.1$		
Fe^{III}-**1**	Gly	692 ± 12	-3.9 ± 0.1		
Fe^{III}-**2**		452 ± 6	-3.6 ± 0.1		
Fe^{III}-**1**	CN^-	$2.9 \times 10^7 \pm 7935$	-10.2 ± 0.4	-19.0 ± 0.8	-28.5 ± 1.0
Fe^{III}-**2**		$1.9 \times 10^6 \pm 4171$	-9.2 ± 0.3	-17.1 ± 0.8	-25.6 ± 1.2
Fe^{III}-**1**	N_3^-	24 ± 1.4	-1.7 ± 0.1		
Fe^{III}-**2**		6.5 ± 0.1	-1.1 ± 0.1		
Fe^{III}-**1**	phenol	12.5 ± 0.7	-1.5 ± 0.1		
Fe^{III}-**2**		4.5 ± 0.2	-0.9 ± 0.1		
Fe^{III}-**1**	fluoride	1.0 ± 0.1	0.0 ± 0.1		
Fe^{III}-**2**		0.9 ± 0.05	$+0.1 \pm 0.1$		

[a] K_{eq} and $\Delta G°$ values at 25 °C for the following ligands were corrected for ligand pK_a via eq 2 (see Experimental Section).

Herein we report the results of a study comparing binding of anionic ligands of widely varying field strength by Fe^{III}-**1** and Fe^{III}-**2**. The key finding in these studies is that weak-field ligands in which the coordinating atom bears a full (fluoride, chloride, hydroxide) or partial (phenoxide, thiocyanate) negative charge causes dissociation of the His ligand in Fe^{III}-**2** but not in Fe^{III}-**1**. The possible role of heme geometry differences in explaining this striking difference in response of Fe^{III}-**1** and Fe^{III}-**2** toward weak-field anions is discussed, as are the strengths and limitations of heme peptides as models of heme proteins.

Experimental Section

Materials. All reagents were of commercial grade and were used without further purification. Preparation of **1** and **2** was accomplished by previously reported methods. It should be noted that **2** exists in two isomeric forms, with the peptide attached to either the 6- or 7-propionate group of heme. Although it has not proven possible to separate these isomers, it is not expected that the different points of attachment will exert a significant effect on heme properties.

Electronic Absorption Spectroscopy. Electronic absorption spectra were recorded on Kontron Uvikon 9410 and Varian Carey 100 Bio UV/vis spectrophotometers. Temperature in the former is controlled by a circulating water bath, and monitored with an Omega Model HH200 thermometer with T thermocouple (±0.2 °C). The latter contains a Peltier-thermostatted cell holder and a dedicated temperature probe accessory (±0.1 °C). A quartz cuvette with 1.0 cm path length was used in all cases. Ligand binding titrations were performed in 60:40 (v/v) H_2O/CH_3OH, buffered to pH 8.0 with 50 mM potassium phosphate. The concentration of Fe^{III}-**1** or Fe^{III}-**2** was held constant at 3−5 μM, while that of the ligand was varied. For all ligands other than cyanide, data were fit to a standard equation describing a 1:1 binding isotherm (eq 1) using the program Igor Pro v.4.0 (Wavemetrics, Inc.), where A_λ is the absorbance at a given wavelength, $A_{\lambda(HP)}$ is the corresponding absorbance for hemepeptide (HP) Fe^{III}-**1** or Fe^{III}-**2** in the absence of ligand, $\epsilon_{\lambda(HP)}$ and $\epsilon_{\lambda(L-HP)}$ are the extinction coefficients at that wavelength in the absence of ligand and in the presence of a saturating concentration of the ligand, respectively, [L] is the concentration of free ligand, and K_d is the dissociation constant. The value of $\epsilon_{\lambda(L-HP)}$ was allowed to vary to obtain the best fit. The extremely tight binding of cyanide necessitated that association constants be obtained via nonlinear regression analysis (Associate v. 1.6)[20] because we could not make the assumption that $[L] = [L]_{bound} + [L]_{free}$ as required in eq 1. Binding constants reported in Table 1 (K) are adjusted for the ligand pK_a: imidazole (7.00), glycine (9.70), phenol (9.99), cyanide (9.21) via eq 2.

$$A_\lambda = A_{\lambda(HP)} - \left[\left(\frac{[HP][L]}{K_d}\right)\Big/\left(1 + \frac{[L]}{K_d}\right)\right](\epsilon_{\lambda(HP)} - \epsilon_{\lambda(L-HP)}) \quad (1)$$

$$K = K_{obs}\left(1 + \frac{[H^+]}{K_a}\right) \quad (2)$$

Electron Paramagnetic Resonance Spectroscopy. X-band EPR spectra were recorded on a Bruker EMX EPR spectrometer equipped with an ER4102ST cavity. An Oxford temperature controller ITC503 with liquid He was used to control sample temperature. Samples were dissolved in 3:1:1 H_2O/CH_3OH/glycerol solution, buffered to pH 8.0 with 100 mM sodium phosphate. Instrumental parameters: microwave power, 2.0 mW at 9.5 GHz; modulation, 10 G at 100 kHz.

Circular Dichroism Spectroscopy. CD spectra were recorded at 25 °C on a Jasco J-710 spectropolarimeter equipped with a Neslab RTE-111 circulating water bath and a Neslab RS232 remote temperature sensor. A 1.0 cm cylindrical, water-jacketed cell was used in all cases. Far-UV spectra (sample concentration 1.8−2.5 μM) are reported in terms of mean residue ellipticity ([θ], in deg·cm^2·dmol^{-1}), calculated as $[\theta] = [\theta]_{obs}(MRW/10lc)$ where $[\theta]_{obs}$ is the ellipticity measured in millidegrees, MRW is the peptide mean residue molecular weight (molecular weight divided by the number of amino acids), c = sample concentration in mg/mL, and l = optical path length of the cell in cm. Soret region spectra (sample concentration 10−12 μM) are reported in terms of molar ellipticity ($[\theta]_{Soret}$, in deg·cm^2·dmol^{-1}), calculated as $[\theta]_{Soret} = [\theta]_{obs}(MW/10lc)$ where MW is the molecular weight of the compound. All spectra represent an average of five scans.

pH Titrations. Alkaline pH titrations of Fe^{III}-**1** and Fe^{III}-**2** were performed on the Uvikon spectrophotometer described above. We used the multicomponent buffer system developed by Munro and Marques[2] for examining the pH-dependent behavior of **1**, comprising CHES, MES, MOPS, potassium hydrogen phthalate, and TRIS (each at 1.0 mM), at a total ionic strength of 0.10M (KCl). Samples of Fe^{III}-**1** and Fe^{III}-**2** (2−3 μM) contained a total volume of 3.0 mL and included 40% (v/v) CH_3OH to prevent aggregation. The pH was adjusted from 8 to 13 in ~0.2 pH increments by adding 1

(20) Peterson, B. R. Ph.D. Thesis. University of California, Los Angeles, Los Angeles, CA, 1994.

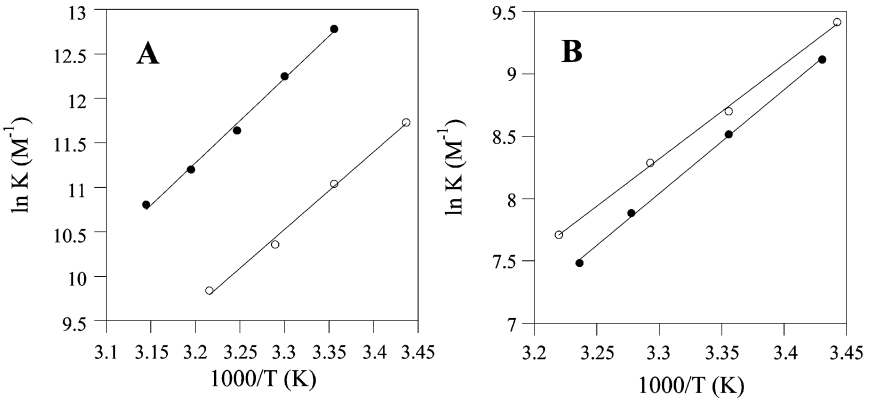

Figure 2. Van't Hoff plots for binding of cyanide (A) and imidazole (B) by Fe^{III}-**1** (●) and Fe^{III}-**2** (○). Titrations were performed in 60:40 (v/v) H_2O/CH_3OH. Solutions were buffered to pH 8.0 with 50 mM potassium phosphate.

M NaOH. The solution was allowed to equilibrate at each pH for 5 min before recording spectra.

Results

Binding Studies with Anionic Ligands Results of our previously reported studies of ImH, Gly, and MTE complexation by Fe^{III}-**1** and Fe^{III}-**2** at 25 °C and pH 8 are reported in Table 1. Also included in Table 1 are results of analogous studies with cyanide, fluoride, azide, and phenol (which binds as the conjugate base phenoxide). Binding studies with each of these ligands are detailed in the following sections, along with attempts to generate the hydroxide complexes of Fe^{III}-**1** and Fe^{III}-**2** by deprotonation of the aquo ligands at elevated pH.

Cyanide. Cyanide is one of the strongest ligands for ferric porphyrins, almost invariably forming low-spin complexes with monohistidine-ligated ferric heme proteins. Cyanide likewise forms very stable, low-spin 1:1 complexes with Fe^{III}-**1** and Fe^{III}-**2** (Table 1; Figures S1 and S2, Supporting Information). Conversion of iron to the low-spin state in Fe^{III}-**1** and Fe^{III}-**2** by cyanide and other strong-field ligands is accompanied by substantial changes in their UV/vis spectra, including a shift of the Soret band λ_{max} to longer wavelength and disappearance of the porphyrin-to-iron charge-transfer band near 620 nm.

In light of the effect of weak-field anionic ligands on Fe^{III}-**2**, described below, it is important to note that cyanide binding by Fe^{III}-**2** does not disrupt peptide helix content, as determined by far-UV CD spectroscopy. In fact, cyanide ligation by Fe^{III}-**2** is accompanied by a small increase in helix content (Figure S3). We consider it likely that this is due to restriction of His side chain conformational freedom, likely arising from shortening of the His−Fe bond upon conversion from the high-spin aquo complex to the low-spin cyanide complex.

Our binding studies showed that cyanide ligates 1.0 kcal/mol more strongly to Fe^{III}-**1** than to Fe^{III}-**2** at 25 °C. Van't Hoff analysis revealed that this arises from an ∼1.9 kcal/mol more favorable binding enthalpy, which is partially offset by a 0.9 kcal/mol less favorable entropy change (Figure 2A; Table 1). The thermodynamic data we obtained for complexation between Fe^{III}-**1** and cyanide in aqueous methanol are similar to previously reported data for the same reaction in aqueous solution.[21]

Fluoride. Fluoride is a much weaker axial ligand than cyanide, and binding studies indicate that fluoride exhibits little difference in affinity for Fe^{III}-**1** and Fe^{III}-**2** (Table 1; Figures S4 and S5). It has previously been demonstrated that displacement of the aquo ligand in Fe^{III}-**1** by fluoride eliminates low-spin iron character, as evidenced by changes in its EPR spectrum recorded in aqueous glycerol.[22] Halide complexes of ferric porphyrins and ferric heme proteins are invariably high-spin, a phenomenon that can be attributed to interactions between the lone pair electrons on the exogenous ligand and electrons in the iron d_{xz} and d_{yz} orbitals, which decrease the energy gap between those orbitals and the $d_{x^2-y^2}$ and d_{z^2} orbitals.[23] We have reproduced the effect of fluoride on the EPR spectra of Fe^{III}-**1** at 11 K in a water/methanol/glycerol mixture (Figure 3A). The EPR spectrum of the Fe^{III}-**1** fluoride complex is virtually identical to that of the Fe^{III}-**2** aquo complex, and converting the aquo complex of Fe^{III}-**2** to a fluoride complex exerts little effect on its EPR spectrum (Figure 3B). Both of these observations are consistent with our previously reported conclusion that Fe^{III}-**2** exhibits very little low-spin character to begin with.

Figure 4A shows that fluoride binding exerts little if any effect on the far-UV CD spectrum of Fe^{III}-**1**. To the best of our knowledge, this is the first conclusive evidence that the His ligand in Fe^{III}-**1** remains ligated to iron following trans coordination of fluoride. Fluoride likewise forms high-spin, six-coordinate complexes with many monohistidine-ligated ferric heme proteins. In marked contrast, reaction between fluoride and Fe^{III}-**2** is accompanied by complete loss of peptide helicity, as determined by far-UV CD (Figure 4C), indicating His ligand dissociation. Fluoride binding by Fe^{III}-**2** also led to disappearance of the Soret band signal (Figure 4D), the source of which is coupling of peptide and porphyrin transition dipoles, but no such loss was observed for Fe^{III}-**1** (Figure 4B).

(21) Blumenthal, D. C.; Kassner, R. J. *J. Biol. Chem.* **1980**, *255*, 5859−5863.
(22) Wang, J.-S.; Tsai, A.-L.; Palmer, G.; Van Wart, H. E. *J. Biol. Chem.* **1992**, *267*, 15310−15318.
(23) Huheey, J. E.; Keiter, E. A.; Keiter, R. L. *Inorganic Chemistry*: *Principles of structure and reactivity*, 4th ed.; Harper Collins College Publishers: New York, 1993.

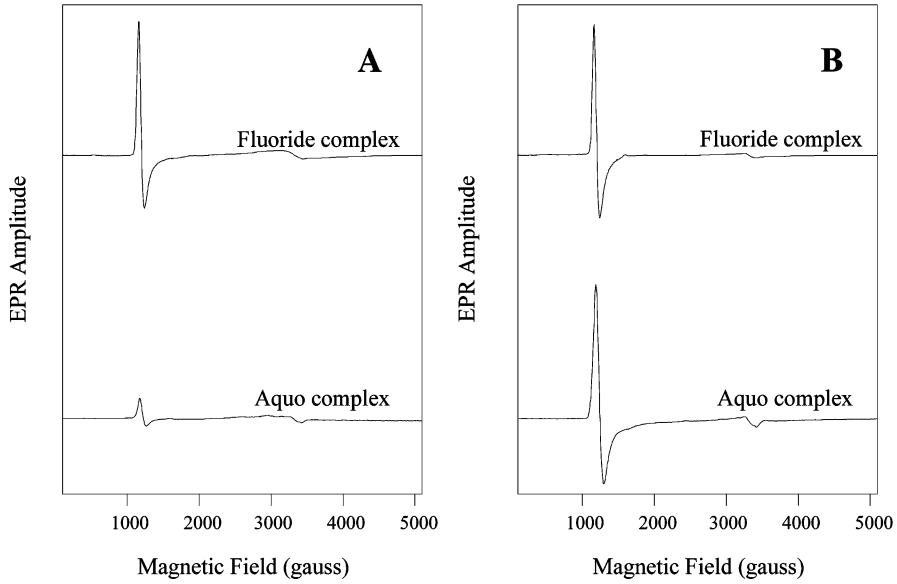

Figure 3. EPR spectra of the fluoride (2M KF) and aquo complexes of Fe^{III}-**1** (A) and Fe^{III}-**2** (B) [each at 35 μM concentration] recorded at 4 K in 3:1:1 water/methanol/glycerol, buffered to pH 8.0 with 100 mM potassium phosphate. The *y* axes in each plot are scaled identically.

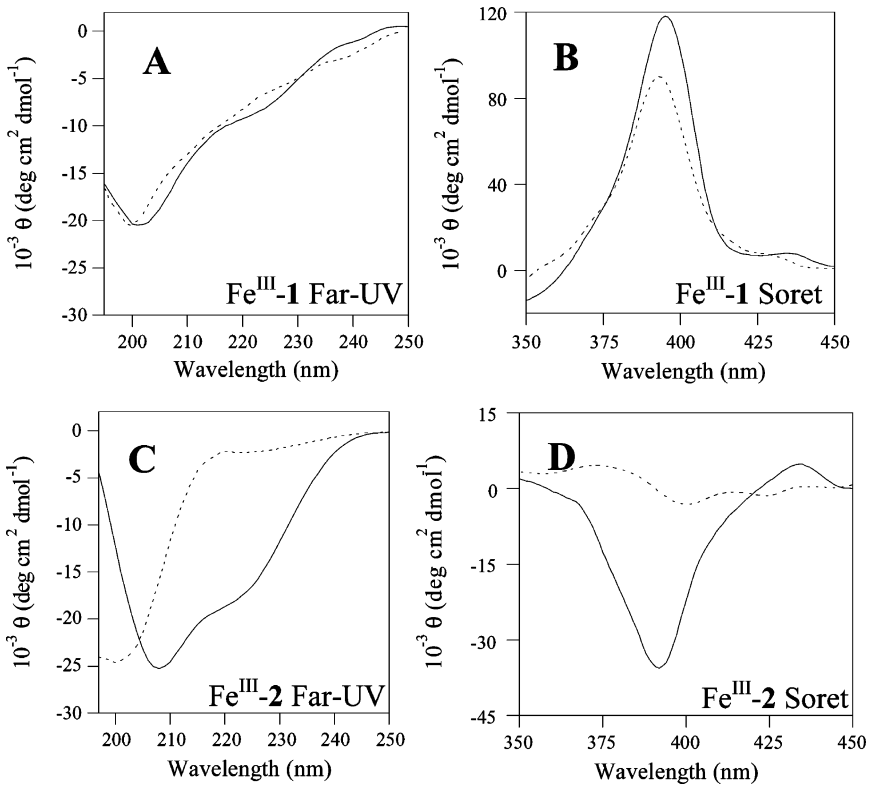

Figure 4. Far-UV (A, C) and Soret region (B, D) CD spectra of the aquo (solid line) and fluoride (dashed line) complexes of Fe^{III}-**1** and Fe^{III}-**2**, respectively. All samples were buffered to pH 7.0 with 50 mM phosphate, and spectra were recorded at 25 °C.

Azide. Azide binds ~4-fold (0.6 kcal/mol) more strongly to Fe^{III}-**1** than to Fe^{III}-**2** (Table 1; Figures S6 and S7). Previous studies with the azide complex of Fe^{III}-**1** in aqueous solution demonstrated the presence of a small amount of high-spin iron in thermal equilibrium with the low-spin form.[24] Consistent with that report, we found that lowering the temperature from 25 to 5 °C led to a small red-shift of the Soret band of the Fe^{III}-**1** azide complex in 60:40 H_2O/CH_3OH, indicating a small increase in low-spin character (Figure 5A). The azide complex of Fe^{III}-**2** also exhibits a high-spin/low-spin thermal equilibrium at 25 °C, but with much greater high-spin character, as evidenced by (1) a much broader Soret band at a given temperature and (2) a much larger red-shift of the Soret band when the temperature is lowered from 25 to 5 °C (Figure 5B).

The azide concentrations required to obtain saturation binding with the two heme peptides prevented us from directly probing its effect on peptide conformation by far-

(24) Marques, H. M.; Cukrowski, I.; Vashi, P. R. *J. Chem. Soc. Dalton Trans.* **2000**.

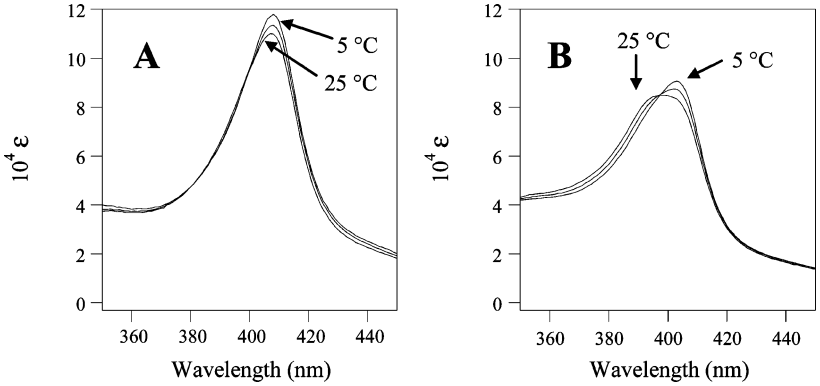

Figure 5. UV/vis spectra of azide (1 M) complexes of Fe^{III}-**1** (A) and Fe^{III}-**2** (B) at 5, 15, and 25 °C. All spectra were recorded in 60:40 CH_3OH/H_2O buffered to pH 7 with 50 mM potassium phosphate.

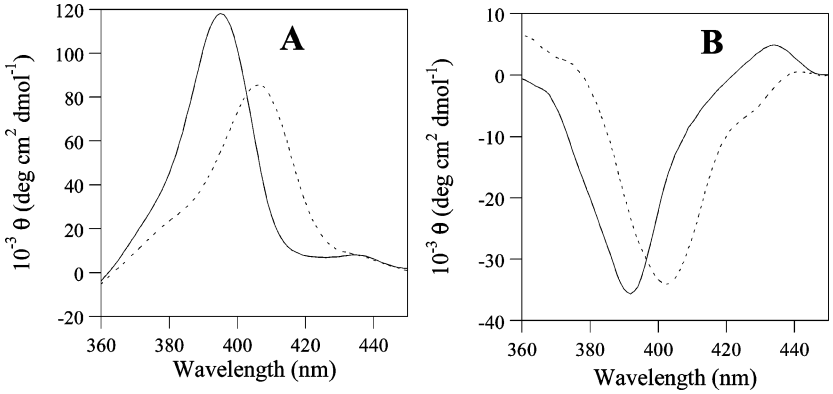

Figure 6. Soret region CD spectra of the aquo (solid line) and azide [1 M] (dashed line) complexes of Fe^{III}-**1** (A) and Fe^{III}-**2** (B) [each at 15 μM]. All samples were buffered to pH 7.0 with 50 mM phosphate and spectra were recorded at 25 °C.

UV CD. However, Soret region CD data strongly suggest that His remains ligated in the azide complexes of both Fe^{III}-**1** (Figure 6A) and Fe^{III}-**2** (Figure 6B). The CD Soret band of the Fe^{III}-**2** azide complex at 25 °C is centered near 403 nm (Figure 6B), corresponding to the λ_{max} of the low-spin form of the complex in UV/vis spectra. The Soret region CD spectrum of the Fe^{III}-**2** azide complex does not contain the distinct shoulder near 391 nm observed in the corresponding UV/vis spectrum, however, which arises from the high-spin form of the complex. Considered in the light of other studies described herein, this suggests that thermal conversion of the low-spin form of the Fe^{III}-**2** azide complex to the high-spin form may be accompanied by His ligand dissociation.

Hydroxide. Deprotonation of the aquo ligand of Fe^{III}-**1** ($pK_a = 9.6$) in aqueous solution has been shown to shift the Soret band λ_{max} from 396 to 398 nm and to modestly decrease the Soret band extinction coefficient.[2] An analogous experiment performed in 60:40 (v/v) CH_3OH/H_2O for the purposes of the present study produced nearly identical results (Figure S8). The small red-shift of the Soret band of Fe^{III}-**1** as the pH is raised above 9.6 has been attributed to an increase in low-spin character of Fe^{III}, consistent with the fact that hydroxide is a stronger-field ligand than water for ferric porphyrins.[25] Fe^{III}-**1**(OH) remains predominantly high-spin, however.[18] Comparison of far-UV and Soret region CD spectra of Fe^{III}-**1** at pH 7 (Figure 7A; solid lines) and 12 (Figure 7A; dashed lines) show that deprotonation of the aquo ligand leaves the His-Fe^{III} bond intact.

An alkaline pH titration performed with Fe^{III}-**2** in 60:40 H_2O/CH_3OH led to a decrease in the Soret band extinction coefficient, but no change was observed in its Soret band λ_{max} (Figure S9). We instead observed emergence of a broad band centered near 350 nm (Figure S9). A similar band is observed in UV/vis spectra of Fe^{III}-**2** and its relatives recorded in H_2O at pH 7 but (1) disappeared when 40% CH_3OH was added as a cosolvent[12] and (2) became less prominent as concentration was lowered.[13,14] These observations strongly suggested that Fe^{III}-**2** engages in self-association via $\pi-\pi$ interactions in neutral aqueous solution. Supporting this conclusion is a report showing that aggregation of Fe^{III}-**1** under high salt conditions also leads to emergence of a band near 350 nm.[26]

Appearance of a band near 350 nm upon aggregation of Fe^{III}-**2** in neutral aqueous solution was not accompanied by disruption of peptide secondary structure, as evidenced in far-UV CD spectra. In contrast, the CD data in Figure 8B show that increasing the pH to 12 in a solution of Fe^{III}-**2** in 60:40 H_2O/CH_3OH leads to complete loss of peptide helicity. On the basis of this observation, we conclude that appearance of a band near 350 nm in the UV/vis spectrum of Fe^{III}-**2** at elevated pH is due to formation of a μ-oxo dimer rather than a hydroxide complex, which like aggregation would bring

(25) Evans, D. R.; Reed, C. A. *J. Am. Chem. Soc.* **2000**, *122*, 4660−4667.

(26) Munro, O. Q.; Marques, H. M. *Inorg. Chem.* **1996**, *35*, 3768−3779.

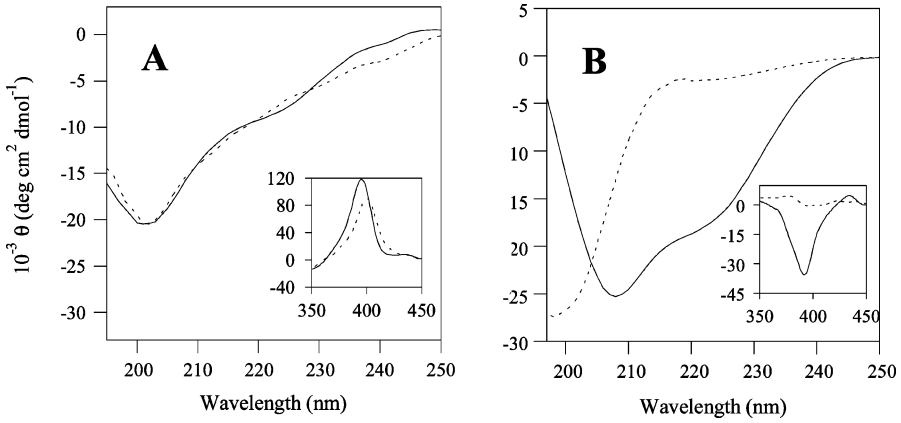

Figure 7. Far-UV CD spectra of Fe^{III}-**1** (A) and Fe^{III}-**2** (B) in 60:40 (v/v) H_2O/CH_3OH at pH 7.0 (solid lines) and 12.0 (dashed lines). Inset: Soret region spectra at pH 7.0 (solid lines) and 12.0 (dashed lines). All spectra were recorded at 25 °C.

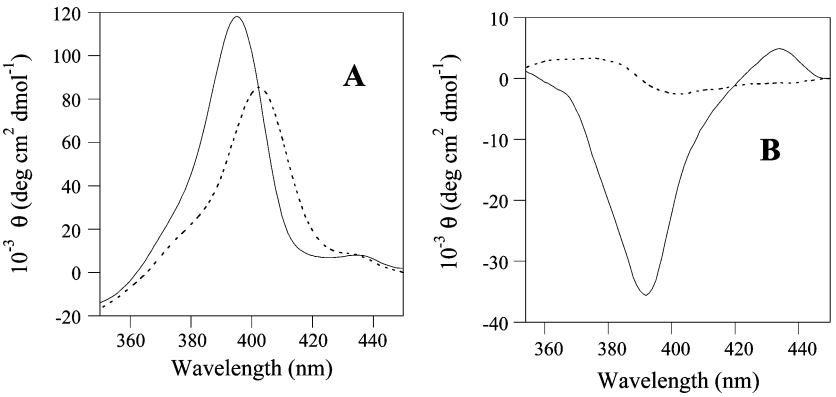

Figure 8. Soret region CD spectra of the aquo (solid line) and phenoxide (dashed line) complexes of Fe^{III}-**1** (A) and Fe^{III}-**2** (B), respectively. All samples were buffered to pH 7.0 with 50 mM phosphate and spectra were recorded in 60:40 (v/v) H_2O/CH_3OH at 25 °C.

the π-systems of two hemes into close contact. When the pH of the sample of Fe^{III}-**2** was lowered from 12 to 7 by addition of acid, the original CD spectrum was recovered, indicating that μ-oxo dimer formation is reversible. In contrast, ferric heme forms μ-oxo dimers in aqueous solution at or below neutral pH, and the process is essentially irreversible because the dimers are insoluble.[27] We attribute reversibility of μ-oxo dimer formation by Fe^{III}-**2** to solubility provided by the pendent peptides, consistent with literature reports showing that μ-oxo dimer formation by water-soluble porphyrins in aqueous solution is also reversible.[28]

Phenoxide. Titrating Fe^{III}-**1** with phenol at pH 8 led to modest changes in its UV/vis spectrum, similar to those observed upon aquo ligand deprotonation and indicative of a small increase in low-spin iron character (Figure S10). Taking into account the fact that the aquo ligand in Fe^{III}-**1**(H_2O) is ~6 orders of magnitude more acidic than free water, we consider it highly likely that phenol ($pK_a = 10$) ligates to both Fe^{III}-**1** and Fe^{III}-**2** in the conjugate base form (phenoxide; PhO^-) at pH 8. Titrating Fe^{III}-**2** with phenol led to more modest spectroscopic changes than were observed for Fe^{III}-**1** (Figure S11), indicating that the resultant complex does not gain significant low-spin character. Phenoxide was found to bind about 4-fold (0.5 kcal/mol) more strongly to Fe^{III}-**1** than to Fe^{III}-**2** but absorbs too strongly in the far-UV region to allow its effect on peptide helix content to be probed directly. However, phenoxide binding leads to complete loss of the CD Soret band in Fe^{III}-**2** but not in Fe^{III}-**1** (Figure 8). It can therefore be concluded that phenoxide is yet another weak-field anion that forces dissociation of the His ligand in Fe^{III}-**2** but not in Fe^{III}-**1**.

Chloride and Thiocyanate. We briefly compared the effects of two additional weak-field anionic ligands, chloride and thiocyanate, on integrity of the His−Fe bond in Fe^{III}-**1** and Fe^{III}-**2**. Rather than perform complete binding titrations, we simply added each ligand in an excess of 1 M. As with all of the other weak-field anionic ligands examined, chloride and thiocyanate binding led to His dissociation in Fe^{III}-**2** but not in Fe^{III}-**1**. For chloride, this could be demonstrated by changes in both far-UV and Soret region CD spectra (Figure S12). Because thiocyanate absorbs strongly in the far-UV region, Soret region CD spectra were used to determine its effects on His ligation in the two heme peptides (Figure S13). On the basis of these findings, we conclude that dissociation of His by weak-field anionic ligands in Fe^{III}-**2** but not in Fe^{III}-**1** is a general phenomenon.

Revisiting Two Key Neutral Ligands. MTE. The results described above for weak-field anionic ligands led us to ponder whether our recently reported[12] failure to observe low-spin Fe^{III} upon binding of the thioether MTE by Fe^{III}-**2** was also due to His dissociation. MTE is another ligand that

(27) Silver, J.; Lukas, B. *Inorg. Chim. Acta* **1983**, *78*, 219−224.
(28) Miller, J. R.; Taies, J. A.; Silver, J. *Inorg. Chim. Acta* **1987**, *138*, 205−214 and references therein.

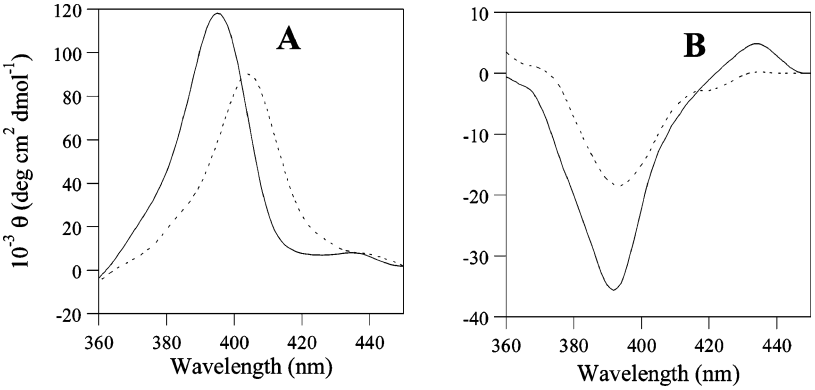

Figure 9. Soret region CD spectra of the aquo (solid line) and MTE [5 M] (dashed line) complexes of Fe^{III}-**1** (A) and Fe^{III}-**2** (B) [each at 15 μM]. All samples were buffered to pH 7.0 with 50 mM phosphate, and all spectra were recorded at 25 °C.

absorbs too strongly to allow us to investigate its effect on His-Fe ligation in Fe^{III}-**1** and Fe^{III}-**2** by far-UV CD spectroscopy. The data in Figure 9A show that MTE ligation to Fe^{III}-**1** causes a red-shift of the Soret band signal and a decrease in molar ellipticity, closely mirroring its effects on Soret band λ_{max} and molar extinction coefficient in UV/vis spectra. The Soret region CD data in Figure 9B show that MTE ligation by Fe^{III}-**2** also leads to a decrease in Soret band molar ellipticity. The CD Soret band of Fe^{III}-**2** does not undergo a red-shift upon MTE ligation, however, consistent with formation of a high-spin complex as our previous studies have indicated.[12] The decrease in CD Soret band molar ellipticity of Fe^{III}-**2** resulting from MTE ligation is considerably larger than the corresponding decrease in Soret band molar extinction coefficient in UV/vis spectra (see Figure S14). This suggests the possibility that displacement of the aquo ligand in Fe^{III}-**2** by MTE leads to partial dissociation of the His ligand, resulting in equilibrium between high-spin His/MTE- and MTE/OH_2-ligated forms. The main argument against this conclusion is that the Soret band in the UV/vis spectrum of Fe^{III}-**2** becomes narrower as [MTE] is increased (see Figure S14), whereas it would more likely broaden if an equilibrium between His/MTE and MTE/OH_2 complexes was achieved, as each would likely have a different Soret band λ_{max} (see section on azide binding above). An alternative possibility was suggested to us by the very high concentration of MTE required to approach saturation binding of Fe^{III}-**2**, which causes a large decrease in overall solution polarity relative to the starting sample containing no MTE. This may alter peptide conformation and/or the extent of peptide/porphyrin interactions in the compounds, which are the sources of the induced Soret band signal in Fe^{III}-**2** and in its complexes in which the axial His ligand remains coordinated. Indeed, it is well-known that signals in CD spectra[29] (including heme peptides)[13,14] are more sensitive to minor structural and conformational alterations than are the corresponding signals in UV/vis spectra. Thus, although we cannot completely discount the possibility that ligation of MTE to iron in Fe^{III}-**2** leads to partial His dissociation, the data clearly show that weak-field neutral ligands have a much lower propensity to cause dissociation of the His ligand in Fe^{III}-**2** than do weak-field anionic ligands.

Imidazole. In our previous report we showed that imidazole exhibits a very small (~0.1 kcal/mol) preference for binding to Fe^{III}-**2** rather than to Fe^{III}-**1**. Van't Hoff analysis has now revealed (Figure 2B; Table 1) that imidazole reacts more exothermically with Fe^{III}-**1** than with Fe^{III}-**2**, albeit to a slightly smaller extent ($\Delta\Delta H° \approx 1.5$ kcal/mol) than observed for cyanide ($\Delta\Delta H° \approx 1.9$ kcal/mol). In contrast to our observations for cyanide, the enthalpic advantage enjoyed by Fe^{III}-**1** for binding of imidazole is slightly overshadowed by a larger entropic penalty in comparison to Fe^{III}-**2**. One possible explanation for this observation derives from the following facts: (1) imidazole is a more sterically demanding ligand than cyanide and (2) heme is ruffled in Fe^{III}-**1** but not in Fe^{III}-**2**. Displacement of the meso carbons in a ruffled heme causes one of the two meso−iron−meso axes on a given face of heme to exhibit a convex curve, while the other meso−iron−meso axis is concave. An imidazole ligand will prefer to be aligned somewhere between the convex meso−iron−meso axis (with the meso carbons sloping away from the ligand) and the point at which the carbon perimeter is in the same plane as the central nitrogens. This is likely to increase the entropic penalty for binding of imidazole relative to cyanide because it restricts free rotation about the Fe−N_{Im} bond.

In 2:1 complexes of unhindered imidazoles (e.g., Im, 1-MeIm) and simple ferric porphyrins, the two ligand planes prefer a parallel or nearly parallel alignment. The lowest energy geometry typically has the ligand planes nearly eclipsed with a given N_p−Fe−N_p axis (the angle between a given ligand plane and the N_p−Fe−N_p axis is defined as φ). A small value of φ introduces steric strain between the porphyrin nitrogens and the C−H groups adjacent to the coordinating nitrogen atom on the ligand but allows stabilizing overlap between ligand pπ and metal pπ orbitals.[30] The least sterically demanding orientation for a given imidazole ligand ($\varphi = 45°$) minimizes ligand−metal orbital overlap.[30] Regardless of the angle φ adopted by two imidazole ligands, a parallel or nearly parallel alignment gives rise to a rhombic heme distortion, manifested in a three-line EPR spectrum.

(29) Eliel, E. L.; Wilen, S. H. *Stereochemistry of Organic Compounds*; Wiley-Interscience: New York, 1994; p 1016.

(30) Scheidt, W. R.; Chipman, D. M. *J. Am. Chem. Soc.* **1986**, *108*, 1163−1167.

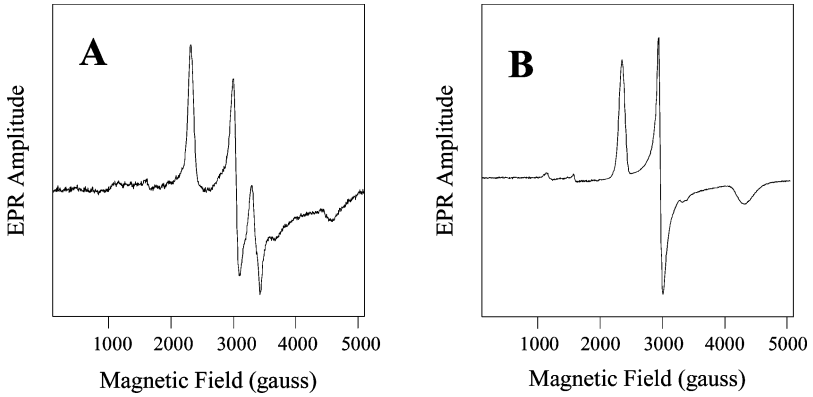

Figure 10. EPR spectra of the imidazole complexes of Fe^{III}-**1** (A) and Fe^{III}-**2** (B) [each at 115 μM] recorded at 11 K in 3:1:1 water/methanol/glycerol, buffered to pH 8.0 with 100 mM potassium phosphate. Each spectrum was recorded in the presence of 200 mM imidazole. The *y* axis scales in the two spectra are identical.

Table 2. EPR Data

	g_x	g_y	g_z
Fe^{III}-**1**(Im)	1.47	2.26	2.92
Fe^{III}-**2**(Im)	1.54	2.28	2.90
D. acetoxicans cyt *c*[32]	1.36	2.27	2.91

If ruffling is sufficiently severe, it can cause a pair of axial imidazole ligands to adopt mutually perpendicular orientations, with the plane of each ligand oriented along the convex meso−iron−meso axis on its side of the porphyrin. Such a ligand arrangement is manifested in EPR spectra dominated by a "large g_{max}" signal at $g > 3.3$.[31] Perpendicular His side chain orientations are observed in a number of bishistidine-ligated *c* cytochromes, a phenomenon likely influenced to some degree by the presence of conserved heme ruffling. It is therefore noteworthy that EPR spectra of Fe^{III}-**1** and Fe^{III}-**2** recorded in the presence of 100 mM ImH at 11 K are remarkably similar and indicative of rhombically distorted heme and therefore of parallel ligand geometry (Figure 10; Table 2). Cyt *c* from *Desulfuromonas acetoxicans* was the first monoheme cyt *c* with bishistidine ligation to be discovered[32] and displays an EPR spectrum nearly identical to those of the imidazole complexes of Fe^{III}-**1** and Fe^{III}-**2** (Table 2). Heme ruffling in bishistidine-ligated cytochromes *c* is therefore not always sufficient to disfavor parallel or nearly parallel His ligand plane alignments.

Virtually no ruffling is observed in two published crystal forms of the ferric tetraphenyl-porphyrin complex [Fe(TPP)-$(Im)_2$]Cl in which the two axial ligands have parallel orientations (both ligands exhibit φ values of 5.7° in one form and 41.4° in the other).[33] In the bisimidazole complex of ferric protoporphyrin IX, the meso carbons alternate ±0.14 Å above and below the mean porphyrin plane,[34] an extent of ruffling that is not sufficient to prohibit the two ligands from adopting an approximately parallel alignment ($\varphi = 16°$ for one ligand and 3° for the other). Ruffling in the originally reported crystal form of [Fe(TPP)$(Im)_2$]Cl is much more significant (meso carbons alternating ±0.3 Å above and below the mean porphyrin plane), and the planes of the two ligands in that complex are rotated in opposite directions relative to one of the N_p-Fe-N_p axes.[35] In other words, this crystal form trends toward the situation encountered in even more highly ruffled low-spin porphyrins which favor perpendicular ligand orientations. That situation is most often associated with sterically hindered ligands such as 2-MeIm, and in fact, substantial ruffling is typically induced by such ligands (meso carbon displacements are ±0.4 Å in the X-ray crystal structure of [Fe(TPP)$(2\text{-MeIm})_2$]ClO_4).[36,37] On the basis of these crystal structure comparisons, we tentatively conclude that heme ruffling in the imidazole complex of Fe^{III}-**1** involves meso carbon displacements of < ±0.3 Å. Displacements of the meso carbon atoms from the mean porphyrin plane in horse heart cytochrome *c*, the source of Fe^{III}-**1**, average ±0.5 Å,[38] and calculations by Shelnutt's group have indicated that removal of Fe^{III}-**1** from its protein context diminishes meso carbon displacement to an average of ±0.36 Å.[9] It is therefore conceivable that complex formation between imidazole and Fe^{III}-**1** is accompanied by a mild *decrease* in heme ruffling.

Discussion

Relationship between Stability and Spin State in Monohistidine-Ligated Heme Proteins. Observations that the hydroxide and phenoxide complexes of Fe^{III}-**1** are predominantly high-spin at pH 7 and 25 °C are interesting in light of the fact that the low-spin state tends to strongly predominate in hydroxide complexes of monohistidine-ligated ferric heme proteins[39] and in the few known examples of natural heme proteins exhibiting His/$TyrO^-$ ligation in

(31) Walker, F. A.; Reis, D.; Balke, V. L. *J. Am. Chem. Soc.* **1984**, *106*, 6888−6898.
(32) Bruschi, M.; Woudstra, M.; Guigliarelli, B.; Asso, M.; Lojou, E.; Petillot, Y.; Abergel, C. *Biochemistry* **1997**, *36*, 10601−10608.
(33) Scheidt, W. R.; Osvath, S. R.; Lee, Y. J. *J. Am. Chem. Soc.* **1987**, *109*, 1958−1963.
(34) Little, R. G.; Dymock, K. R.; Ibers, J. A. *J. Am. Chem. Soc.* **1975**, *97*, 4532−4539.
(35) Collins, D. M.; Countryman, R.; Hoard, J. L. *J. Am. Chem. Soc.* **1972**, *94*, 2066−2072.
(36) Scheidt, W. R.; Kirner, J. F.; Hoard, J. L.; Reed, C. A. *J. Am. Chem. Soc.* **1987**, *109*, 1963−1968.
(37) Walker, F. A.; Huynh, B. H.; Scheidt, W. R.; Osvath, S. R. *J. Am. Chem. Soc.* **1986**, *108*, 5288−5297.
(38) Jentzen, W.; Ma, J.-G.; Shelnutt, J. A. *Biophys. J.* **1998**, *74*, 753−763.
(39) La Mar, G. N.; Satterlee, J. D.; De Ropp, J. S. *Nuclear Magnetic Resonance of Hemoproteins*; Academic Press: New York, 2000; Vol. 5.

the ferric state: the hemophore HasA from *Serratia marcescens*[40] and cytochrome cd_1 nitrite reductase (heme *d*) under physiological conditions,[41] and *Chlamydomonas* chloroplast Hb under alkaline conditions.[42] One factor possibly contributing to this apparent discrepancy is that OH^- and $TyrO^-$ ligands in heme proteins typically reside in low-polarity environments, whereas OH^- and PhO^- ligands to Fe^{III}-**1** are able to engage in hydrogen-bonding interactions with bulk solvent that can weaken their ligand strength. Such an argument has been used to explain the observation that the hydroxide complex of heme oxygenase exhibits a thermal spin equilibrium.[43] The OH^- ligand in this complex is thought to engage in strong hydrogen bonding with a highly organized network of water molecules in the distal pocket.

We have provided evidence that the failure of MTE to convert iron in Fe^{III}-**2** to the low-spin state at pH 7 and 25 °C is due in large measure to insufficiently strong coordination of His, with weak binding of MTE also playing a role.[12] We therefore propose that weak His−Fe ligation in comparison to naturally occurring His-ligated heme proteins likewise contributes to the predominantly high-spin states displayed by the hydroxide and phenoxide complexes of Fe^{III}-**1**. In this context, it is noteworthy that high-spin His−Fe^{III}−OTyr ligation is observed in the β subunits of the clinically important Hb mutant Hb M Saskatoon, in which the distal His residues have been replaced by Tyr (the presence of Tyr strongly favors the Fe^{III} oxidation state under physiologically relevant conditions).[44] The analogous mutations in sperm whale Mb[45] and horse heart Mb[46,47] also produced high-spin His−Fe^{III}−OTyr ligation. The fact that these mutants are not low-spin is likely due to the location of the Tyr residue, which may not allow its side chain to form a sufficiently strong Fe^{III}−O bond. Indeed, the angle between the Tyr and heme planes in the H64Y Mb mutants is much larger than the corresponding angle in HasA and cyt cd_1.

In Hb M Boston, the distal His residues in the α subunits are replaced by Tyr, which again stabilizes Fe^{III} relative to Fe^{II}. Ligation of the distal Tyr side chains to heme iron in Hb M Boston results in displacement of the proximal His ligands,[44,48] analogous to the effect of phenoxide on Fe^{III}-**2**. The difference in response of the α and β subunits of Hb to the distal His to Tyr mutation is consistent with (1) the fact that iron is further displaced from the heme plane in the α subunits of deoxyHb than from the β subunits,[49] and the His−Fe bonds in those subunits are consequently more strained, and (2) the observation that cyanide introduced into crystals of T-state metHb bound to Fe^{III} in all four subunits, causing dissociation of the proximal His ligands in the α subunits but not in the β subunits.[50]

The only confirmed example of a natural heme protein exhibiting His ligand dissociation following deprotonation of a trans aquo ligand is the ferric form of the homodimeric Hb from the blood clam *Scapharca inaequivalvis*.[51] While it is not clear whether this phenomenon has physiological relevance, together with the Hb M Boston example it demonstrates that rupture of His-Fe bonds by weak-field anionic ligands is not a phenomenon that is restricted to simple model compounds such as Fe^{III}-**2**.

Why Do Only Weak-Field Anions Rupture the His-Fe Bond in Fe^{III}-2? Scheidt et al. have reported the X-ray crystal structure of the ferric octaethylporphyrin complex [Fe(OEP)(2-MeIm)ClO_4], the only example of a five-coordinate ferric porphyrin in which the single axial ligand is neutral.[52] Iron in this complex is displaced 0.34 Å from the plane defined by the four pyrrole nitrogen atoms. Somewhat smaller out-of-plane displacement is observed for the five-coordinate, monohistidine-ligated ferric ion in *Aplysia limacina* metMb (0.26 Å)[53] and in five-coordinate mammalian metMb mutants (e.g., 0.28 Å in the H64T mutant of horse metMb).[54] The out-of-plane displacements in these and other high-spin ferric porphyrins are stabilizing because they relieve overlap between filled orbitals centered on the pyrrole nitrogens and the singly occupied iron $d_{x^2-y^2}$ orbital.[55,56] A wide variety of crystal structures have been reported for five-coordinate ferric porphyrins in which the sole axial ligand is an anion, including fluoride, chloride, bromide, iodide, alkoxides, phenoxides, thiophenoxides, thiocyanate, and azide.[57] Crystal structures of two ferric porphyrin μ-oxo dimers have also been reported.[58,59] In the vast majority of these five-coordinate complexes, Fe^{III} is displaced from the mean porphyrin plane to a greater extent (0.4−0.6 Å) than in [Fe(OEP)(2-MeIm)ClO_4] and in the five-coordinate metMbs noted above. Scheidt and co-workers attributed the larger displacing effect of anionic ligands to the fact that

(40) Arnoux, P.; Haser, R.; Izadi, N.; Lecroisey, A.; Delepierre, M.; Wandersman, C.; Czjzek, M. *Nat. Struct. Biol.* **1999**, 6, 516−520.
(41) Williams, P. A.; Fülöp, V.; Garman, E. F.; Saunders, N. F. W.; Ferguson, S. J.; Hajdu, J. *Nature* **1997**, *389*, 406−412.
(42) Das, T. K.; Couture, M.; Lee, H. C.; Peisach, J.; Rousseau, D. L.; Wittenberg, B. A.; Wittenberg, J. B.; Guertin, M. *Biochemistry* **1999**, *38*, 15360−15368.
(43) Caignan, G. A.; Deshmukh, R.; Zeng, Y.; Wilks, A.; Bunce, R. A.; Rivera, M. *J. Am. Chem. Soc.* **2003**, *125*, 11842−11852.
(44) Jin, Y.; Nagai, M.; Nagai, Y.; Nagatomo, S.; Kitagawa, T. *Biochemistry* **2004**, *43*, 8517−8527.
(45) Egeberg, K. D.; Spring, B. A.; Martinis, S. A.; Sligar, S. G.; Morikis, D.; Champion, P. M. *BIochemistry* **1990**, *29*, 9783−9791.
(46) Maurus, R.; Bogumil, R.; Luo, Y.; Tang, H.-L.; Smith, M.; Mauk, A. G.; Brayer, G. D. *J. Biol. Chem.* **1994**, 269.
(47) Tang, H.-L.; Chance, B.; Mauk, A. G.; Powers, L. S.; Reddy, K. S.; Smith, M. *Biochim. Biophys. Acta* **1994**, *1206*, 90−96.
(48) Pulsinelli, P. D.; Perutz, M. F.; Nagel, R. L. *Proc. Natl. Acad. Sci. U.S.A.* **1973**, *70*, 3870−3874.
(49) Robinson, V. L.; Smith, B. B.; Arnone, A. *Biochemistry* **2003**, *42*, 10113−10125.
(50) Paoli, M.; Dodson, G.; Liddington, R. C.; Wilkinson, A. J. *J. Mol. Biol.* **1997**, *271*, 161−167.
(51) Das, T. K.; Boffi, A.; Chiancone, E.; Rousseau, D. L. *J. Biol. Chem.* **1999**, *274*, 2916−2919.
(52) Scheidt, W. R.; Geiger, D. K.; Lee, Y. J.; Reed, C. A.; Lang, G. *J. Am. Chem. Soc.* **1985**, *107*, 5693−5699.
(53) Bolognesi, M.; Onesti, S.; Gatti, G.; Coda, A. *J. Mol. Biol.* **1989**, *205*, 529−544.
(54) Bogumil, R.; Maurus, R.; Hildebrand, D. P.; Brayer, G. D.; Mauk, A. G. *Biochemistry* **1995**, *34*, 10483−10490.
(55) Scheidt, W. R.; Lee, Y. J. *Struct. Bonding* **1987**, *64*, 1−70.
(56) Scheidt, W. R.; Reed, C. A. *Chem. Rev.* **1981**, *81*, 543−555.
(57) Scheidt, W. R. Systematics of the stereochemistry of porphyrins and metalloporphyrins. In *The Porphyrin Handbook*; Kadish, K. M.; Smith, K. M.; Guilard, R., Eds. Academic Press: San Diego, 2000; Vol. 3, pp 49−112.
(58) Hoffman, A. B.; Collins, D. M.; Day, V. W.; Fleischer, E. B.; Srivastava, T. S.; Hoard, J. L. *J. Am. Chem. Soc.* **1972**, *94*, 3620−3626.
(59) Cheng, B.; Hobbs, J. D.; Debrunner, P. G.; Erlebacher, J.; Shelnutt, J. A.; Scheidt, W. R. *Inorg. Chem.* **1995**, *34*, 102−110.

Fe(porph)X complexes are neutral whereas the corresponding imidazole-ligated complexes retain a formal +1 charge on iron.[52] This positive charge was thought to increase Coulombic attraction between Fe^{III} and the porphyrin ring, which bears two formal negative charges, with the result that Fe^{III} is held closer to the porphyrin center. The iron atom in six-coordinate high-spin ferric porphyrins has less flexibility insofar as venturing from the heme plane is concerned, as highlighted in recently published high-resolution crystal structures of horse aquometHb[49] and sperm whale aquomet-Mb.[60] In both proteins, Fe^{III} is displaced from the porphyrin plane in the direction of the stronger ligand His, but only by 0.11−0.14 Å. Fe^{III} is also displaced from the porphyrin plane in the six-coordinate H64Y mutants of metMb noted above. The extent of the displacement in the H64Y metMb mutants is significantly larger, however, (∼0.34 Å) and is in the direction of the anionic tyrosinate ligand.

On the basis of the above considerations, we propose the following explanation for the differences in effects exerted by weak-field neutral ligands and weak-field anionic ligands on Fe^{III}-**2**. His is a stronger ligand than the neutral species H_2O and MTE and therefore will form a stronger bond with the iron atom. As a result, iron in the aquo and MTE complexes of Fe^{III}-**2** will tend to be displaced at least a small distance toward His. The crystallographic data discussed herein show that anions, even if weaker Lewis bases than His, tend to pull high-spin Fe^{III} further out of plane. This can be expected to cause a lengthening of the His−Fe bond, which would tend to favor His dissociation. Furthermore, out-of-plane iron displacement by both neutral and anionic ligands is commonly associated with a doming distortion of the porphyrin, in which the four pyrrole rings tilt away from the ligand (Figure 1C and D).[57] Doming of the porphyrin in Fe^{III}-**2** following anion ligation would render the entire His-ligated face of the heme concave, an effect that is likely to further encourage His dissociation by increasing steric strain between the porphyrin and the ligand.

Why Do Fe^{III}-1 and Fe^{III}-2 Differ in Their Response to Weak-Field Anionic Ligands? We contend that the remarkable ability of the His ligand in Fe^{III}-**1** to resist dissociation following coordination of a weak-field anionic ligand cannot be simply due to the fact that the His-ligated form of Fe^{III}-**1** is 0.7−1.4 kcal/mol more stable than the His-ligated form of Fe^{III}-**2**. The basis for this contention is that displacement of the aquo ligand by fluoride in Fe^{III}-**2** converts the heme peptide from a state in which the His-ligated form is ∼3 kcal/mol more stable than the His-dissociated form[12] to one in which it is at least 95% His-dissociated (unfolded form >2.7 kcal/mol more stable than the folded form). The change from a neutral to an anionic weak-field ligand therefore diminishes the stability of the His-ligated form of Fe^{III}-**2** by nearly 6 kcal/mol. This greatly exceeds the 0.7−1.4 kcal/mol greater stability exhibited by Fe^{III}-**1** relative to Fe^{III}-**2**.

As discussed in the introduction, one of the few other significant differences exhibited by these two heme peptides is that heme in Fe^{III}-**1** is ruffled, whereas heme in Fe^{III}-**2** is not. Recall that ruffling creates a convex meso−iron−meso axis on each side of the heme and adjacent concave meso−iron−meso axes. A convex axis should provide the opportunity for His to move closer to the porphyrin than is possible in a planar His-ligated ferric porphyrin, thereby allowing iron to be displaced to some extent in the direction of the anionic ligand without straining the His−Fe bond to the extent that requires bond rupture. Moreover, heme ruffling in Fe^{III}-**1** enforced by the structural features of the molecule is likely to prevent significant doming that could *increase* His/porphyrin steric interactions by rendering the His-ligated face of the heme concave.

Concluding Remarks

We have now identified three complexes of Fe^{III}-**1** and Fe^{III}-**2** that exhibit distinctly different thermal spin equilibria, with the complex of Fe^{III}-**1** displaying greater low-spin character in each case. In two of the complexes, the second axial ligand is a weak-field neutral species (H_2O; MTE), while in the third, the ligand is an anion with a moderately strong ligand field (N_3^-). As already proposed on the basis of the aquo and MTE complexes,[12] this is almost certainly due in large measure to tighter binding of both the intramolecular and exogenous ligands in the Fe^{III}-**1** complexes. Similarly, we contend that the stronger ligand binding that is possible in heme proteins in comparison to heme peptides contributes to the fact that hydroxide and phenoxide form predominantly high-spin complexes with Fe^{III}-**1**, whereas His−Fe^{III}−OH and His−Fe^{III}−OTyr ligation in proteins typically produces a low-spin state. In short, our results indicate that differences in heme binding affinities by the apo forms of heme protein variants is an important mechanism by which heme spin properties can be modulated. This complements other research in our laboratories indicating that variation in heme binding affinity is one of the major factors governing redox potentials of heme protein variants having identical axial ligation.[61,62]

The major finding in this study is that weak-field anionic ligands force the rupture of the His−Fe bond in Fe^{III}-**2** but not in Fe^{III}-**1**. We have attributed this to the fact that heme is ruffled in Fe^{III}-**1** but likely planar in Fe^{III}-**2** with the potential to become domed. While anion-induced His ligand dissociation is not a common occurrence in heme proteins, we are aware of two established examples: Hb M Boston ($TyrO^-$ ligation) and *Aplysia limacina* Hb at elevated pH (OH^- ligation). It is interesting to consider the possibility that heme geometry also plays a role in these phenomena. For example, anion-induced His ligand dissociation in heme proteins could result if the prosthetic group resided in a flexible region of the protein. This could allow the porphyrin to dome after an anion binds to iron and pulls it out of plane,

(60) Vojtechovsky, J.; Chu, K.; Berendzen, J.; Sweet, R. M.; Schlichting, I. *Biophys. J.* **1999**, *77*, 2153−2174.

(61) Cowley, A. B.; Kennedy, M. L.; Silchenko, S.; Lukat-Rodgers, G. S.; Rodgers, K. R.; Benson, D. R. *Inorg. Chem.* **2006**, *45*, 9985−10001.

(62) Kennedy, M. L.; Silchenko, S.; Houndonougbo, N.; Gibney, B. R.; Dutton, P. L.; Rodgers, K. R.; Benson, D. R. *J. Am. Chem. Soc.* **2001**, *123*, 4635−4636.

thereby favoring His dissociation by introducing steric strain as we have proposed for Fe^{III}-**2**.

Finally, the results reported herein emphasize the difficulty in accurately recapitulating ligation and spin properties of natural heme proteins in synthetic heme peptides and their complexes, despite success in our group and by others in endowing heme peptides with protein-like structural features as demonstrated by NMR[63,64] and more recently by X-ray crystallography.[65] Even cyt *c* heme peptides are not always equal to the task, as illustrated by the fact that the hydroxide and phenoxide complexes of Fe^{III}-**1** are predominantly high-spin. Our studies show, however, that comparison of structurally similar heme peptides can provide insight into heme protein structure/function/stability relationships that are difficult to achieve in investigations of the natural systems.[61,62] We feel that the work related herein shows that studies comparing synthetic heme peptides such as **2** with heme peptides derived from cytochrome *c* can be particularly beneficial, as they allow insight into the consequences of one of nature's well-known "design" strategies: introducing a double covalent polypeptide−heme linkage into cytochrome *c*, which forces the porphyrin to undergo a ruffling distortion. In future studies, we intend to pursue the following hypothesis which arose from the work described herein: that introducing heme ruffling into synthetic heme peptides will make ligation and spin-state properties of their complexes with weak-field exogenous ligands more like those of natural heme proteins.

Acknowledgment. The work reported herein was supported by a grant from the Petroleum Research Fund (AC-3477).

Supporting Information Available: Various spectral data. This material is available free of charge via the Internet at http://pubs.acs.org.

IC060682C

(63) Liu, D.; Williamson, D. A.; Kennedy, M. L.; Williams, T. D.; Morton, M. M.; Benson, D. R. *J. Am. Chem. Soc.* **1999**, *121*, 11798−11812.
(64) D'Auria, G.; Maglio, O.; Nastri, F.; Lombardi, A.; Mazzeo, M.; Morelli, G.; Paolillo, L.; Pedone, C.; Pavone, V. *Chem. Eur. J.* **1997**, *3*, 350−362.
(65) Costanzo, L.; Geremia, S.; Randaccio, L.; Nastri, F.; Maglio, O.; Lombardi, A.; Pavone, V. *J. Biol. Inorg. Chem.* **2004**, *9*, 1017−1027.